Water Science & Technology

IWA PUBLISHING

Water Science & Technology Vol 84 No 3, 538 doi: 10.2166/wst.2021.253

Application of artificial neural network (ANN-MLP) for the prediction of fouling resistance in heat exchanger to MgO-water and CuO-water nanofluids

Ahmed Benyekhlef[a,*], Brahim Mohammedi[b], Djamel Hassani[a] and Salah Hanini[a]

[a] Laboratory of Biomaterials and Transport Phenomena (LBMPT), University of Medea, Medea, 26000, Algeria
[b] Nuclear Research Center of Birine, Djelfa, 17000, Algeria
*Corresponding author. E-mail: benyekhlefahmed80@gmail.com

ABSTRACT

In this work, an artificial neural network (ANN) model was developed with the aim of predicting fouling resistance for heat exchanger, the network was designed and trained by means of 375 experimental data points that were selected from the literature. These data points contain six inputs, including time, volumetric concentration, heat flux, mass flow rate, inlet temperature, thermal conductivity and fouling resistance as an output. The experimental data are used for training, testing and validation of the ANN using multiple layer perceptron (MLP). The comparison of statistical criteria of different networks shows that the optimal structure for predicting the fouling resistance of the nanofluid is the MLP network with 20 hidden neurons, which has been trained with Levenberg–Marquardt (LM) algorithm. The accuracy of the model was assessed based on three known statistical metrics including mean square error (MSE), mean absolute percentage error (MAPE) and coefficient of determination (R^2). The obtained model was found with the performance of {MSE $= 6.5377 \times 10^{-4}$, MAPE $= 2.40\%$ and $R^2 = 0.99756$} for the training stage, {MSE $= 3.9629 \times 10^{-4}$, MAPE $= 1.8922\%$ and $R^2 = 0.99835$} for the test stage and {MSE $= 5.8303 \times 10^{-4}$, MAPE $= 2.57\%$ and $R^2 = 0.99812$} for the validation stage. In order to control the fouling procedure, and after conducting a sensitivity analysis, it found that all input variables have strong effect on the estimation of the fouling resistance.

Key words: artificial neural networks, fouling, graphical user interface, heat exchanger, modeling, nanofluid

HIGHLIGHTS

- Reduction of fouling resistance in heat exchangers.
- A high determination coefficient has been reached ($R^2 = 0.99770$).
- Developing a program and an interface to facilitate the calculation for users.

ABBREVIATIONS

A_f	Accuracy factor
ANN	Artificial neural network
B_f	Bias factor
b_i	Bias values of hidden layer
b_j	Bias value of output layer
C	Volumetric concentration [%]
FR	Fouling resistance [m^2 K·KW^{-1}]
G	Mass flow rate [$Kg.m^{-2}$ S^{-1}]
I_j	Relative importance of the input variable
K, K'	Criteria of acceptability
MAPE	Mean absolute percentage error
MLP	Multi layer perceptron
MSE	Mean squared error
N_h	Number of neurons in the hidden layer
q	Heat flux, [KW·m^{-2}]
RMSE	Root mean squared error
R^2	Coefficient of determination
t	Time [h]
T	Temperature [°C]

Ts Surface (wall) temperature [°C]
W_{ij} Synaptic weights between the hidden layer and the output layer

Super/Subscripts

exper Experimental value
max Maximum
min Minimum
pred Predicted value

Greek symbols

λ Thermal conductivity [$W{\cdot}m^{-1}{\cdot}K^{-1}$]

1. INTRODUCTION

Surface fouling reduces the performance of various types of process equipment such as heat exchanger, contamination of nuclear reactors or blockage of membrane filters, reverse osmosis units, which are used in desalination, power generation, and water and wastewater treatment plants. Combating the fouling of process equipment costs industries billions of dollars each year, and can render some processes uneconomic which are otherwise technologically and environmentally viable. Particulate fouling has also been the subject of many investigations and various models have been proposed to predict the extent of particulate fouling in process equipment.

In the literature, there are few articles published to identify the fouling phenomenon and its impacts, namely a comprehensive study presented in literature review regarding mitigation and retardation of fouling and particles deposition in heat exchanger presented in recent experimental and numerical studies investigated by various researchers (Awais & Bhuiyan 2019). Williamson *et al.* (1988) studied the deposition of haematite (α–Fe_2O_3) particles suspended in water and found that the deposition is dependent on the suspension pH. Grandgeorge *et al.* (1998) performed an experimental study on the liquid–phase particulate fouling using deionized water containing TiO_2 particles as a foulant fluid in stainless steel plate heat exchangers. (Peyghambarzadeh *et al.* 2012) studied the deposition of micron–sized α–alumina particles which are introduced into a hydrocarbon base fluid (n–heptane). The deposition during forced convection heat transfer is measured using an accurate thermal approach. Furthermore, new theoretical model has been developed to predict the asymptotic fouling resistance. An experimental study to examine the role of generating bubbles on fouling on the heat transfer surface in an annular heat exchanger, a systematic comparison is performed to study the effect of bubble generation in the sub-cooled flow boiling regime on the crystallization and particulate fouling (Peyghambarzadeh *et al.* 2013). Nikkhah *et al.* (2015) performed an experimental study in conventional vertical annulus to see the influence of heat, mass flow, wall temperature, concentration of nanofluids, and sub-cooled level on the fouling resistance parameter and heat transfer coefficient of CuO/water. A new correlation for estimating the fouling resistance of nanoparticles based on the isothermal diffusive condition is proposed. Teng *et al.* (2017) studied the deposition of artificially-hardened calcium carbonate in a double-pipe heat exchanger, and simulated a real case of plant operational process related to the heat exchanger equipment. Wang *et al.* (2019) applied an experimental method by changing the concentration, heat flow, mass flow and inlet temperature of the suspensions, to study the effects of particulate fouling on heat transfer under sub-cooled flow boiling using magnesia particulate suspension of which the particle sizes are 40 nm and 10 μm, respectively. An experimental study has been done on the fouling characteristics of the γ-Al_2O_3/water suspension on a surface of stainless steel by changing the heat flux and the inlet temperature under single-phase flow and sub cooled-flow boiling conditions, with mechanism analysis by a visible spectrophotometer (Wang *et al.* 2018). (Sarafraz & Hormozi 2014) shown that fouling resistance represents the linear/asymptotic behavior with time in force convective and nucleate boiling heat transfer regions, by studying experimentally the influence of different operating parameters such as dilute concentrations of nanofluid (by weight), heat flux and mass flux on the single phase, two-phase flow-boiling and particulate fouling resistance of CuO/EG nanofluid. Artificial neural network (ANN) technique has been used in many scientific domains such as (solar, nucleate boiling, solubility of solid drugs, methodology, biofuels, micropollutants) (Laidi and Hanini 2013; Mohamedi *et al.* 2015; Rezrazi *et al.* 2016; Abdallahelhadj *et al.* 2017; Ammi *et al.* 2020; Belmadani *et al.* 2020), and it has proven its reliability and robustness by establishing the relationship between the variables without considering the detailed physical process. This feature of ANN encourages its use for predicting thermophysical properties of nanofluids. In addition, a few, if any, investigations on fouling resistance estimation in heat exchanger using nanofluids were found throughout the literature.

The aim of this work is to develop an ANN-MLP model to predict fouling resistance of nanofluids (MgO-water and CuO-water) in heat exchanger from experimental data based on: time, volumetric concentration, heat flux, mass flow rate, inlet temperature, thermal conductivity. So, this study allows us, on one hand, to determinate the effect of each input parameters on fouling resistance, especially the effect of different particle concentrations; and on other hand, validating the accuracy of the developed ANN-MLP model compared to the proposed correlations in the literature.

2. ARTIFICIAL NEURAL NETWORKS MODEL

Artificial neural network is a new approach for simulating linear and nonlinear system with high complexity in various fields of science and engineering. An artificial neural network consists of large number of processing elements called neurons. They are joined by connecting links called weights. For the design of an efficient artificial neural network, we needed to choose: an input layer, an output layer, an hidden layer, number of neurons in the hidden layer, transfer function, number of hidden layers and learning algorithm. The network performance is determined by the value of weights and biases in every single neuron. The network should be trained using measured data sets to give the desired output following input data sets (Kiani *et al.* 2010; Mohanraj *et al.* 2012).

The ANN based MLP architecture is shown in Figure 1. MLP is an interconnection of perceptrons in which data and calculations flow in a single direction, from the input data to the outputs. The number of layers in an ANN is the number of layers of perceptrons. The output from a given neuron is calculated by applying a transfer function to a weighted summation of its input to give an output, which can serve as input to other neurons (Kumari *et al.* 2014).

The MLP structure consists of three layers: input, hidden, and output layers. They are created by many interconnected neurons. Each layer consists of a weight matrix, some artificial neurons and biases added for each neuron to find an output vector (Bouali *et al.* 2020).

Table 1 shows the range of inputs and output variables.

The input and output data were normalized within the range of [$y_{min} = -1$, $y_{max} = 1$] using a mapminmax algorithm given by Equation (1) that performs a normalization of the maximum and minimum values of each row (Demuth and Beale 2009).

$$y = map\,\min\max(x) = \frac{(y_{max} - y_{min})(x - x_{min})}{(x_{max} - x_{min})} + y_{min} \tag{1}$$

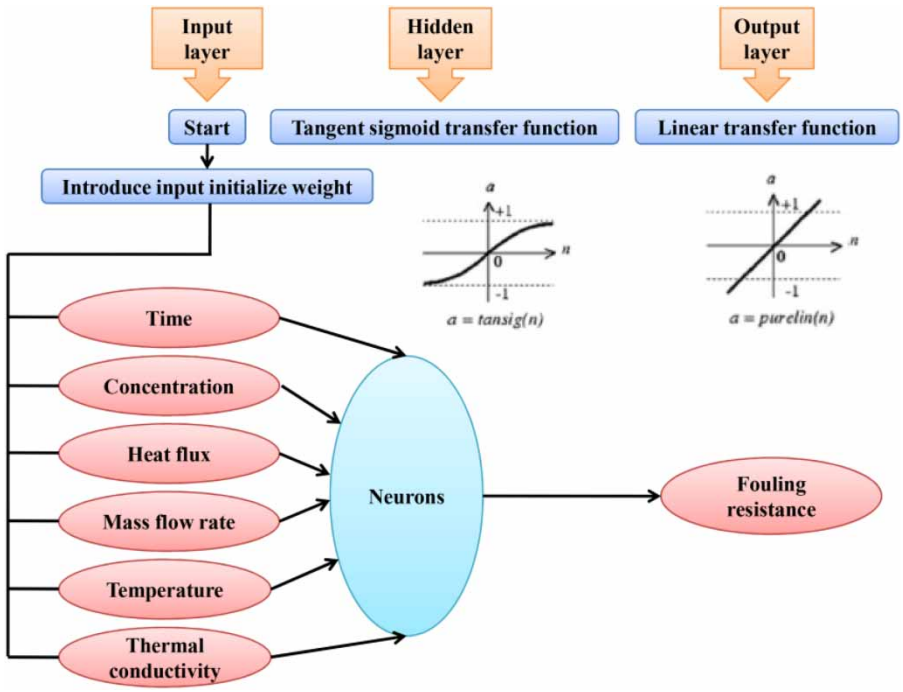

Figure 1 | Architecture of the proposed ANN-MLP model to predict FR.

Table 1 | Range of variables

Parameter		Unit	Min	Max
Time	t	[h]	0,120	26,189
Volumetric concentration %	C	–	0,1	0,4
Heat flux	q	[KW·m^{-2}]	23,6	800
Mass flow rate	G	[Kg·m^{-2}·s^{-1}]	40	80
Inlet temperature	T	[°C]	33	84
Thermal conductivity	λ	[W·m^{-1}·K^{-1}]	18	60
Fouling resistance	FR	[m^2 K·KW^{-1}]	0,0168	1,9794

After examining a considerable number of differently structures neural networks,the optimization of ANN parameters is performed by minimizing the mean absolute percentage error (MAPE), the adequate ANN selected in this paper have a single hidden layer with 30 neurons and an output layer with one neuron. The hidden layer has a tangent sigmoid transfer function (Matlab code: tansig). The output layer has a linear transfer function (Matlab code: purelin). Typical structure of the ANN is shown in Figure 1.

The mathematical formula that connects the inputs to the output of the optimized neural network (ANN) is given in Equation (2).

$$Output = FR = \sum_{N=1}^{N}\left[W_{ij(1.N)}\left(\frac{2}{1+\exp\left(-2\left(\left(\sum_{m=1}^{m} W_{i(N.m)}In_{(m)}\right)+b_{i(N)}\right)\right)}-1\right)\right]+b_j \tag{2}$$

W_{ij} and W_i are the synaptic weights between the input layer and the hidden layer and between the hidden layer and the output layer, respectively; b_i and b_j are the bias vectors of the hidden layer and output layer.

3. MODEL INPUT PARAMETERS AND ERRORS

In order to predict physical properties with ANN-MLP type using experimental results, 375 data for fouling resistance are divided into three sections: training (300 data), testing (37 data) and validation (38 data). Training, testing and validation subsets of the ANN-MLP are obtained as selecting 80% of the dataset as training, 10% of the dataset as testing and 10% of the dataset as validation subsets.

The test and validation data is used to assess the structure of the ANN-MLP type. Testing and validation the model built with training data: to obtain proper polynomial relations for the thermophysical properties of the MgO-water and CuO-water nanofluids regarding the input data, three criteria are used for simulation assessment and comparison between the model results and experimental data. These criteria are: mean square error (MSE), mean absolute percentage error (MAPE) and coefficient of determination (R^2) which can be calculated as follows:

$$MSE = \frac{1}{N}\sum_{i=1}^{N}(y^{\exp}-y^{cal})^2 \tag{3}$$

$$MAPE(\%) = \frac{100}{N}\sum_{1}^{N}\frac{|y^{\exp}-y^{cal}|}{y^{\exp}} \tag{4}$$

$$R^2 = 1-\frac{\sum_{1}^{N}(y_i^{\exp}-y_i^{cal})^2}{\sum_{1}^{N}(y_i^{\exp}-y_i^{\overline{\exp}})^2} \tag{5}$$

Ross (1996) proposed two different indices for determining the performance of the model. The bias factor B_f Equation (6) is a measure of the overall agreement between the predicted and the observed values. It will indicate whether, and to what

extent, the forecasts are above or below the equivalence line. A perfect agreement between the observed and the predicted values would give a B_f of 1. ($B_f = 0.9$–1.05 good model).

The A_f accuracy factor is based on an equation similar to Equation (6) but does not know if the difference between the predicted and the observed values is positive or negative. It shows the spread of results.

$$B_f = 10^{\left(\frac{\sum_{i=1}^{N} \log \frac{y_i^{cal}}{y_i^{\exp}}}{N}\right)} \tag{6}$$

$$A_f = 10^{\left(\frac{\sum_{i=1}^{N} \left|\log \frac{y_i^{cal}}{y_i^{\exp}}\right|}{N}\right)} \tag{7}$$

In addition, to ensure greater validity of the models developed, we used some statistical criteria as follows:

$$K = \frac{\sum y_i^{cal} y_i^{\exp}}{\sum (y_i^{cal})^2} \tag{8}$$

$$K' = \frac{\sum y_i^{cal} y_i^{\exp}}{\sum (y_i^{\exp})^2} \tag{9}$$

where:

$0.85 \leq K \leq 1.15$; $0.85 \leq K' \leq 1.15$ as an acceptability criteria

where $y_i^{\exp}$ representing either the i^{th} trained, test or validation output value and y_i^{cal} representing the corresponding experimental value, with N being the number of input vectors.

4. RESULTS AND DISCUSSION

In this paper, the performance of ANN with varying number of neurons (1–30) in the hidden layer was investigated where each ANN-MLP architecture was trained 15 times in order to avoid random effects. Results demonstrated that architectures with one hidden layer were able to reach the goal in term of errors and determination coefficient. Table 2 shows the result of statistical performance of the ANN model. The accuracy of the networks was evaluated for each epoch in the training through MSE. The best validation performance is 10^{-4} at epoch (iterations) 1,000 for the best network topology with overall MAPE of 2.4535%, % RMSE of 2.54%, values of bias factor $B_f = 1$ and accuracy factor $A_f = 1$, which indicates that the model is valid in the predicting of FR. The values of K and K' indicates that the model is acceptable (Benimam *et al.* 2020).

Figure 2 shows a comparison between experimental and predicted values of fouling resistance during training, test and validation stage. There is very good agreement between target data and the results obtained from the ANN-MLP model. The R^2

Table 2 | Statistical performance of the ANN model

	MAPE (%)	MSE	RMSE	A_f	B_f	K	K'	R^2
Training	2.4054	6.5377e-04	0.0256	1	1	0.9991	0.9999	0.99756
Testing	1.8922	3.9629e-04	0.0199	1	1	0.9995	0.9993	0.99835
Validation	2.5700	5.8303e-04	0.0241	1	1	0.9982	1.0010	0.99812
All	2.3714	6.2119e-04	0.0249	1	1	0.9990	1	0.99770

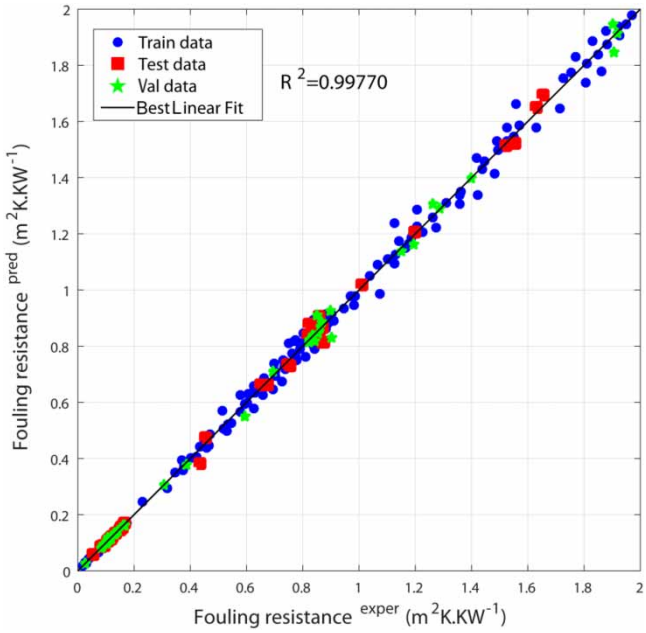

Figure 2 | Experimental vs. predicted fouling resistance (all data sets).

value for the fouling resistance is superior to 0.99 for the training, validation and test data sets showing that the model has captured the features quite accurately. Results confirm the high ability of the used ANN-MLP model and demonstrate a good fitting between the predicted and the experimental values of fouling resistance.

The residual of the predicted values of the fouling resistance against the experimental values for the present model is shown in Figure 3. As most of the calculated residuals are distributed on two sides of the zero line, a conclusion may be drawn that there is no systematic error in the development of the present model.

After the network has been created and all weights and biases were initialized by the use of the ANN-MLP model, the network becomes ready to be trained. During the training, the weights and biases of the network were systematically updated to

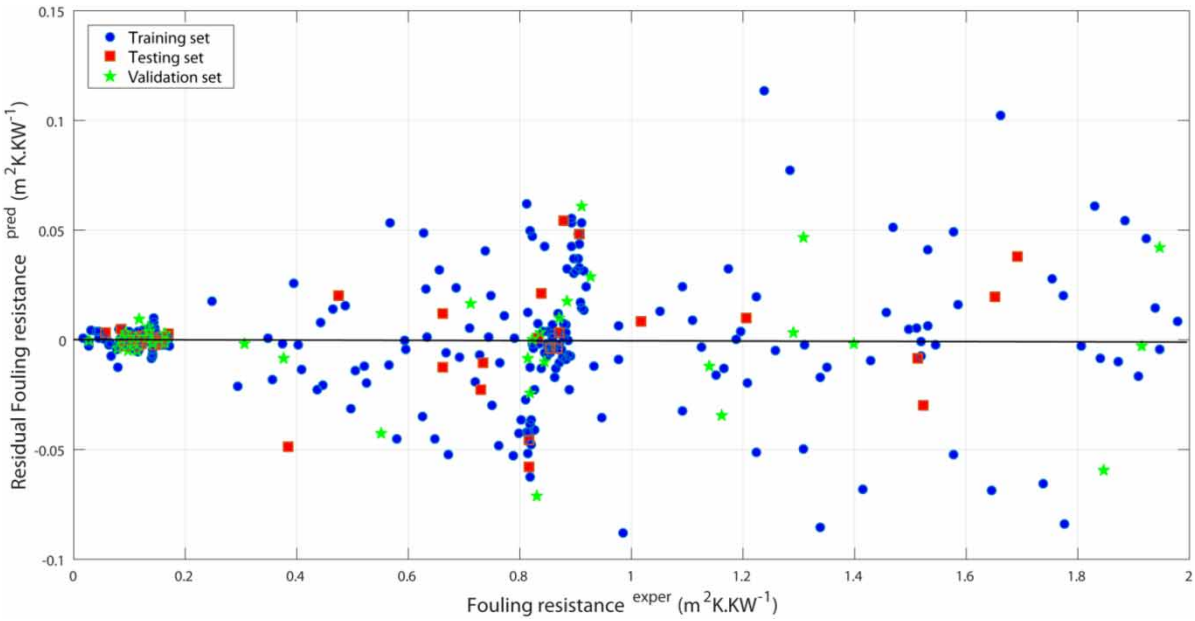

Figure 3 | Plot of the residuals for calculated values of fouling resistance FR from the ANN-MLP model versus their experimental values for the training, testing and validation sets.

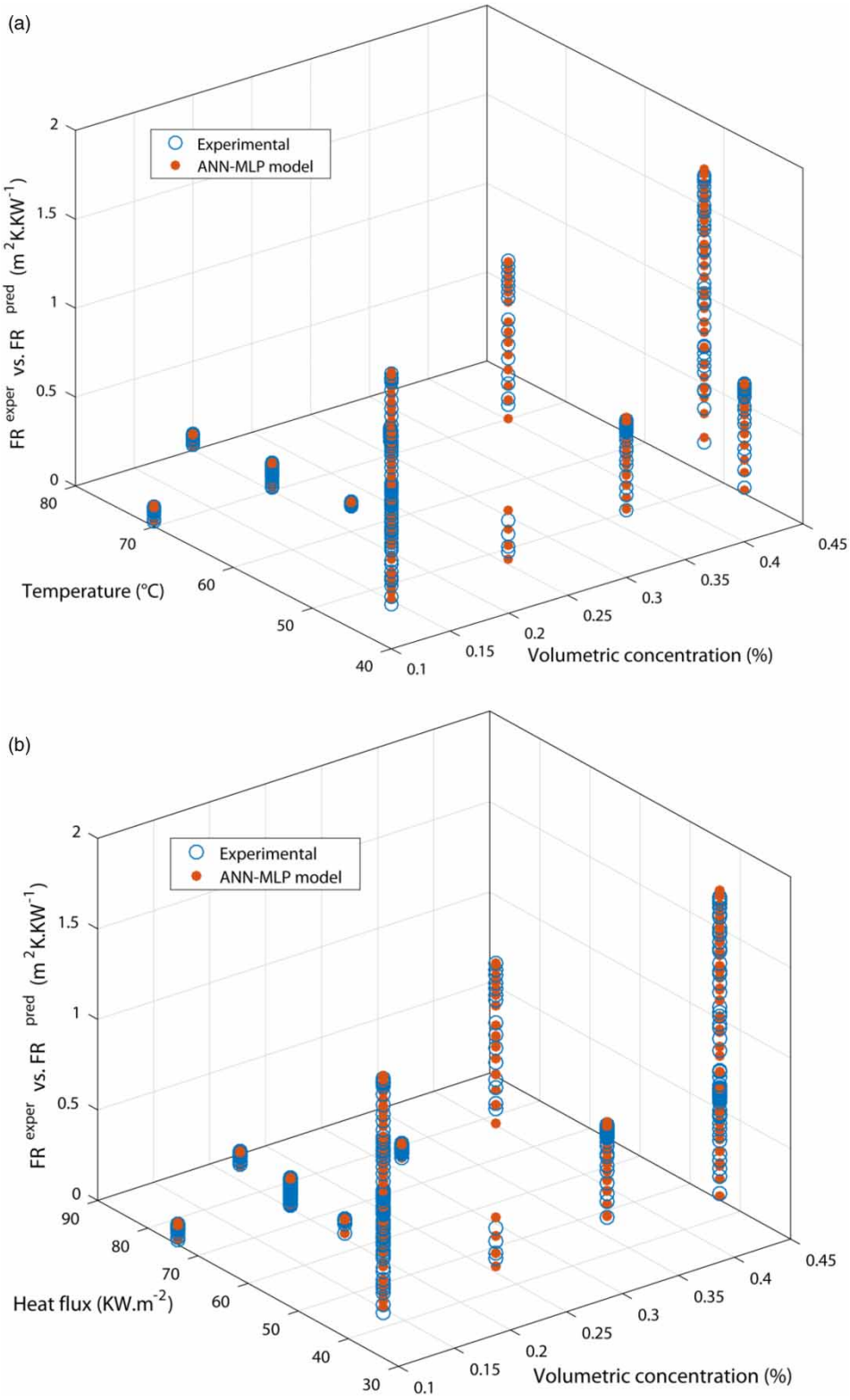

Figure 4 | Distribution of all data sets (a, b, c, and d) between experimental and ANN-MLP predicted of fouling resistance versus inputs parameters. (*Continued*.)

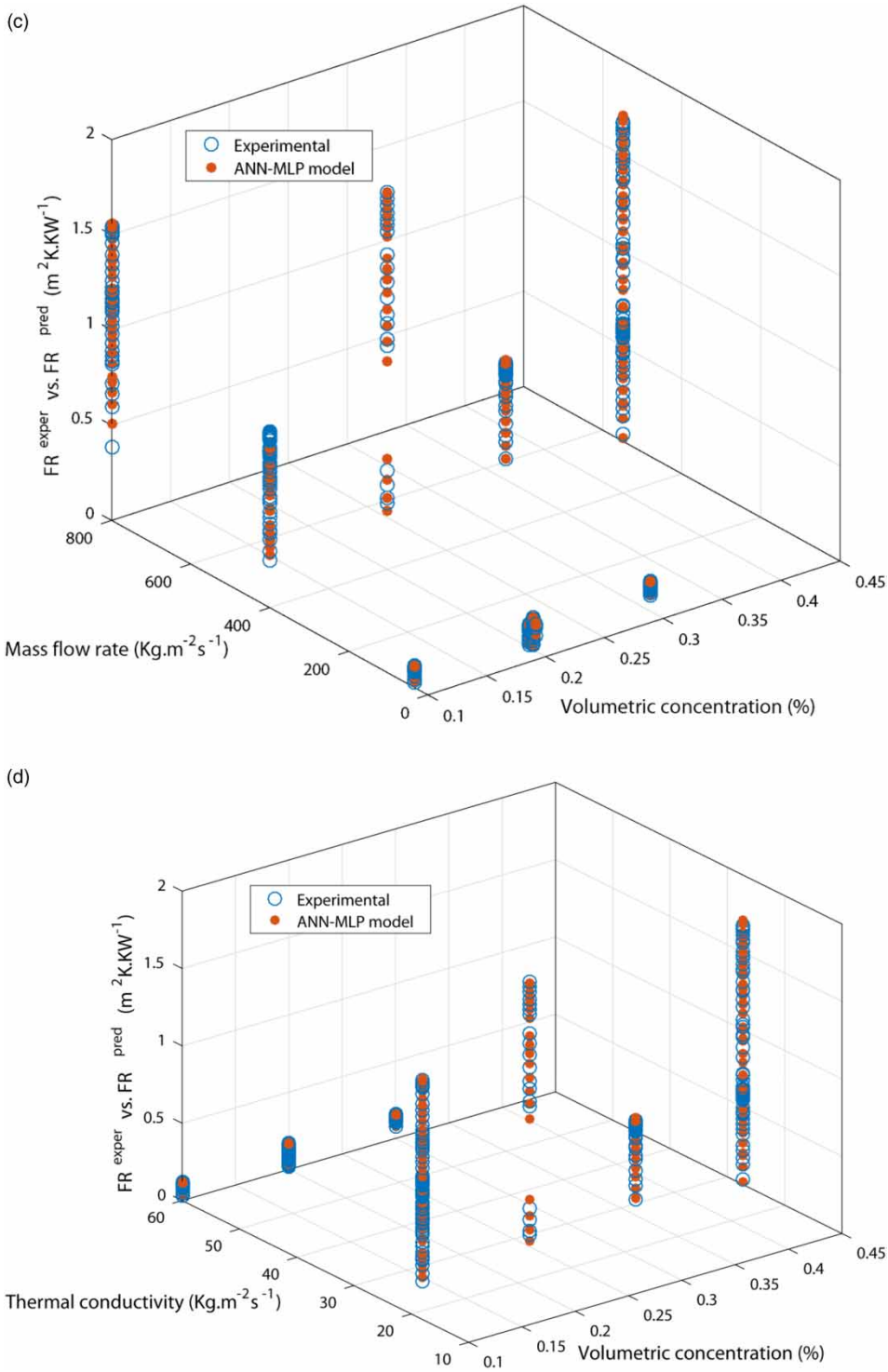

Figure 4 | Continued.

minimize a performance function of MSE in this work between the predicted (target) output and the network output (Soleimani *et al.* 2013). For better visualization, Figure 4 shows the three-dimensional plots of distribution of all experimental data sets compared with ANN-MLP predicted data of fouling resistance of nanofluids (MgO-water and CuO-water) in heat exchanger, and it confirms an excellent prediction performance of ANN-MLP.

4.1. Optimal configuration of neural network prediction model

The optimal configuration of neural network prediction depends on the number of hidden neurons, activation function, learning rate and population size (Tang *et al.* 2020).

The trial-and-error method is used to determine the optimal number of neurons. With the increase of the number of neurons, the prediction accuracy of the neural network is significantly improved. In this work, the number of neurons is varied from 1 to 30, and the effect of the number of neurons on MSE and R^2 is shown in Figure 5. It can be seen that as the number of neurons increases, the MSE decreases and R^2 gradually increases. In order to ensure the prediction accuracy of the neural network, the best network selected is the network with 20 neurons in a hidden layer.

The error comparison results of different training algorithms are shown in Figure 6. It can be seen that the Levenberg-Marquart algorithm has the lowest MSE value and the highest R^2 value. Therefore, the Levenberg-Marquart algorithm is selected in this paper as a training algorithm of the neural network.

4.2. Validation of ANN model

To validate our developed ANN-MLP model, a rough comparison between results of proposed correlation with experimental data of (Nikkhah *et al.* 2015) for nanofluid at volumetric concentration 0.4% by weight and at two different temperature surfaces (wall), the comparison is shown in Figure 7. We can see the precision and the validity of the neural model developed for the prediction of fouling resistance during the flow of nanofluid in heat exchanger.

4.3. Determination of importance of each input variable

In order to investigate the impacts of the inputs parameters selected at the predicted outputs, a sensitivity study is performed, where the model that was chosen to be an application example of the study has six inputs, one output and 20 neurons in its hidden layer; it uses the Min–Max method as a normalization technique and 'Trainlm' as a training algorithm. The matrix of neural network weights in Table 3 can be used to determine the relative importance of various input variables on the output variable.

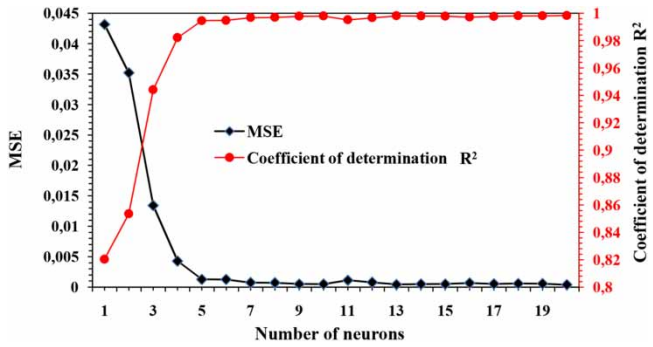

Figure 5 | The effect of neuron number on MSE and R^2.

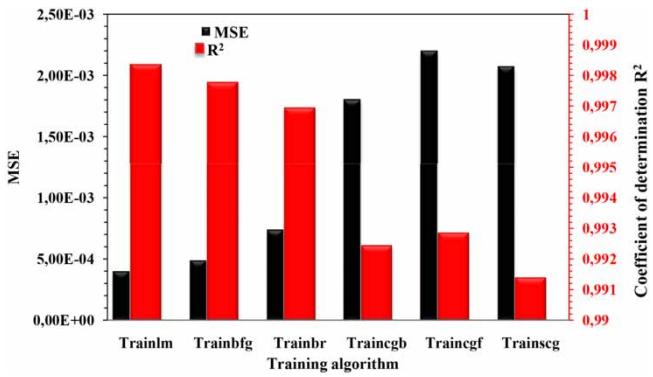

Figure 6 | The effect of training algorithm on MSE and R^2.

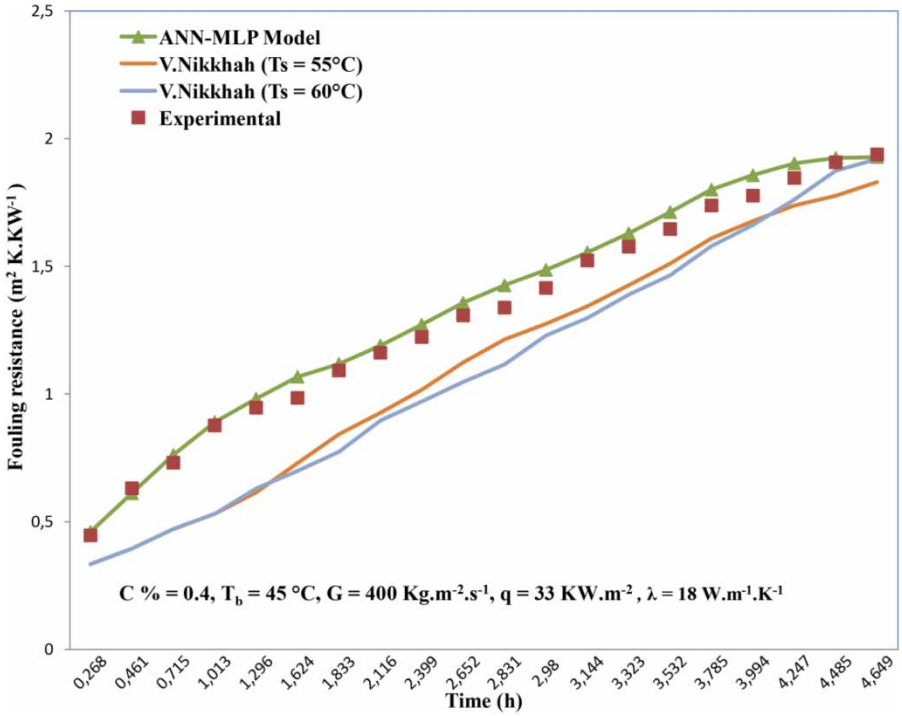

Figure 7 | Comparisons of ANN prediction of FR with experimental data of nanofluid (CuO-water) and empirical correlations in heat exchanger.

Garson (1991) proposed an equation based on partitioning of connection weights:

$$I_J = \frac{\sum_{m=1}^{m=N_h} \left(\left(|w_{j_m}^{i_n}| / \sum_{k=1}^{N_i} |w_{k_m}^{i_h}| \right) \times |w_{m_n}^{h_0}| \right)}{\sum_{k=1}^{k=N_i} \left\{ \sum_{m=1}^{m=N_h} \left(\left(|w_{j_m}^{i_n}| / \sum_{k=1}^{N_i} |w_{k_m}^{i_h}| \right) \times |w_{m_n}^{h_0}| \right) \right\}} \tag{10}$$

where I_j is the relative importance of the j^{th} input variable on output variable; N_i and N_h are the number of input and hidden neurons, respectively; w is connection weights; the superscripts i, h and o refer to input, hidden and output layers, respectively; and subscripts k, m and n refer to input, hidden and output layers, respectively (Garson 1991).

The relative importance of input variables calculated by Equation (10) is shown in Figure 8. It can be seen that logically the various input variables have a strong effect on the fouling resistance.

According to the results, it can be seen clearly that all variables chosen as inputs have a large effect on fouling resistance with very similar proportions. The inlet temperature appears to be the most influential variable (18.29%) followed by heat flux (18.05%) since they improves chemical and crystallization reactions (Kukulka and Devgun 2007; Setoodeh *et al.* 2015), and also increase the motion of particles at the near wall region and strengthened transport (Prodanovic *et al.* 2002). Thermal conductivity comes in third ranking (17.81%); its effect can be related to the nature of material surfaces. Smooth materials with low thermal conductivity have a tendency of providing lower fouling resistance than rough materials with high thermal conductivity (Al-Janabi *et al.* 2011; Ghahdarijani *et al.* 2017). The time with 17.63% of importance has also a significant effect on fouling resistance, because the continuous formation of larger agglomerated particles, sedimentation of instable particle increases, which decreases the thermal conductivity of nanofluids (Al-Janabi *et al.* 2011; Ghahdarijani *et al.* 2017). Mass flow rate contributing 14.22% relative importance on fouling resistance, this is mainly due to shear force across the wall. Knowing that the asymptotic value of fouling resistance decreased gradually when the mass flow rate was increased, this one enhanced the kinetic energy of particles in the working fluid, so, the collision probability increased and promoted agglomeration of particles. As a result, the agglomerated particles were hard to transport to the wall (Peyghambarzadeh

Table 3 | The weight and bias values of each layer determined using optimum ANN-MLP network

	IW{1.1}						b{1}	LW{2.1}	b{2}
Number of neurons	Time	Volumetric concentration	Heat flux	Mass flow rate	Inlet temperature	Thermal conductivity	1	Fouling resistance	2
1	0.03824	− 0.00337	0.08964	0.01764	0.06472	0.01024	2.30152	0.27324	0.02670
2	−0.07627	−0.00255	−0.00960	0.07997	0.06803	0.03703	−2.06285	−0.21286	
3	0.05660	−0.02655	0.10080	−0.00724	0.04699	0.04197	1.81084	0.23622	
4	−0.72509	−0.43681	1.07781	−0.08223	0.15910	−0.48041	0.96047	−0.39881	
5	−8.19613	−2.71585	1.99234	0.91850	−1.12335	−1.07998	−9.08576	2.86256	
6	−0.34532	−0.98860	−0.43978	0.15854	−0.44154	−0.57649	−0.40645	1.46076	
7	−8.74456	−0.39974	1.80089	0.82643	−0.01131	−3.34021	−7.92236	−2.21943	
8	−0.15460	−2.98357	0.39406	0.44654	−1.18418	−0.13286	−1.16851	−1.07664	
9	10.58433	−4.27753	−5.14578	−1.28542	0.20744	1.98948	7.76020	1.15509	
10	−10.14369	−5.07401	−1.14196	−7.91266	4.84281	7.62904	3.97105	−1.35075	
11	−4.22376	−2.40902	0.55248	1.46030	1.95510	3.33504	1.62353	−6.04152	
12	1.81115	0.22668	−2.51267	−0.20894	−0.60086	1.04547	1.29239	5.36764	
13	9.04397	1.86464	−6.96010	1.57880	−1.24683	−1.41260	8.22601	−5.03703	
14	5.82220	0.25384	0.08034	0.70562	−3.12399	−4.01836	−3.04655	−5.48297	
15	10.91474	1.43822	2.71586	−0.27689	0.74697	2.37565	13.65974	3.15974	
16	1.60177	−0.34321	1.10016	−1.39425	1.38939	1.64980	3.33523	−1.87202	
17	−0.11956	1.28735	0.44296	−0.34866	1.11601	0.29405	1.79225	−2.45023	
18	0.00750	−0.18695	−0.04343	0.03493	0.17718	0.07431	−1.75716	0.02865	
19	−0.10405	−0.06723	−0.04608	0.06244	0.00414	0.02780	−2.05720	−0.28809	
20	0.02252	0.01498	0.06651	−0.01164	0.00281	0.02880	2.30316	0.23449	

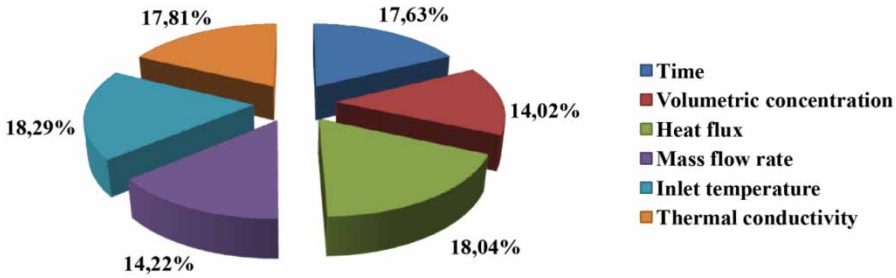

Figure 8 | Relative importance (%) of input variables on the value of the calculated the fouling resistance.

et al. 2013; Zhan *et al.* 2016). The last parameter is the volumetric concentration which imparted 14.02% importance. As stated in Ojaniemi *et al.* (2012); Awais & Bhuiyan (2019), the increase in concentration also increased the contact frequency between the wall and particles and the contact among particles in the main flow, which accelerated the deposition rate. Therefore, it becomes easier for particles to agglomerate and form large particles.

Weight and bias matrix are given in Table 3.

4.4. Program for fouling resistance

A computer program has been developed in MATLAB for the purpose of using the ANN-MLP model for quick and easy calculation of fouling resistance in heat exchangers with more flexibility. This gives the user all the necessary inputs for the execution of model (t: time, C: volumetric concentration, q: heat flux, G: mass flow rate, T: temperature, λ: thermal conductivity) to predict the fouling resistance in heat exchangers during flow of nanofluid Figure 9.

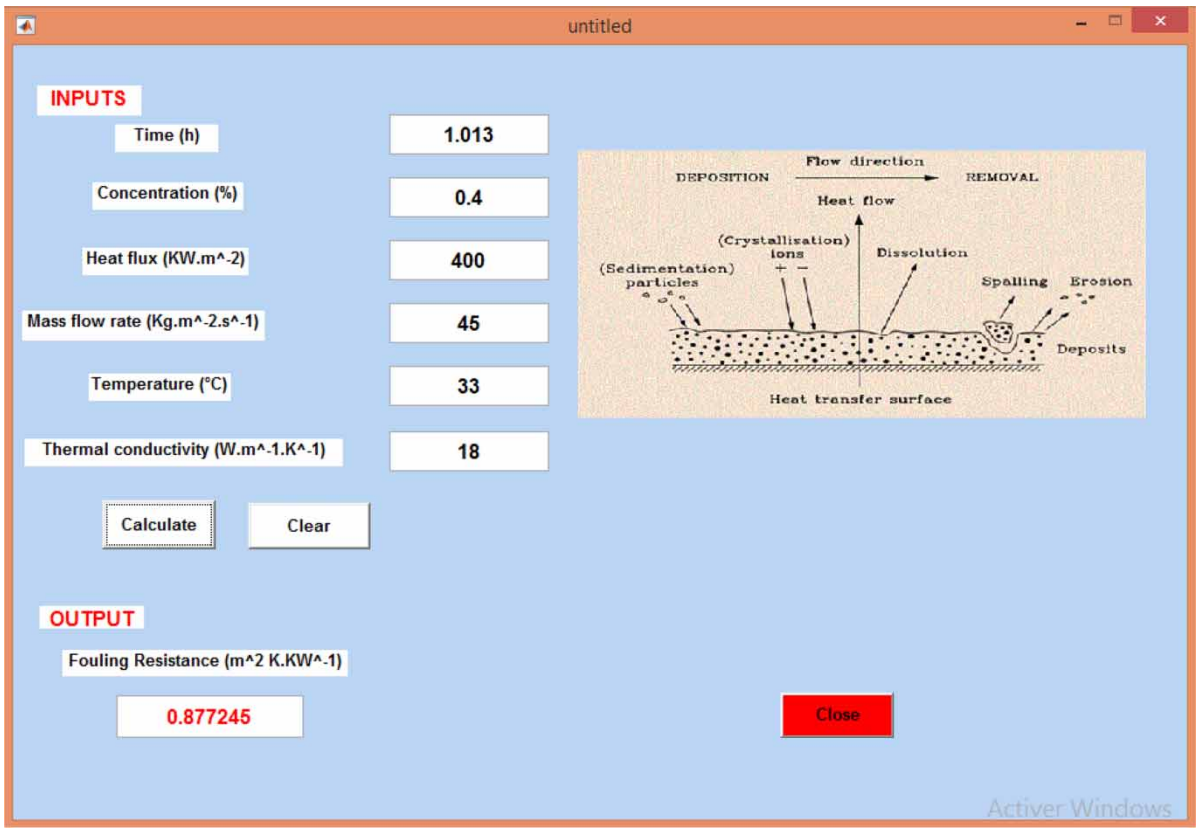

Figure 9 | MATLAB interface for fouling resistance.

5. CONCLUSION

In this work, we developed an ANN-MLP neural network model for the prediction of the fouling resistance during flow of nanofluid in the heat exchanger, depending on the fundamental variables of operating systems such as time, particle concentration, heat flux, mass flow rate, inlet temperature and thermal conductivity under the influence of fouling particulate and deposits. The ANN-MLP is used to estimate the fouling resistance of nanofluid based on experimental data. A total of 375 experimental data points were collected from the literature and divided into three sections: training, testing and validation data. Networks with different structures were compared with experimental data and were assessed based on the various statistical criteria. The proposed ANN-MLP architecture for the estimation of fouling resistance with one hidden layer and 20 neurons in each layer, which was trained with LM algorithm and the tangent sigmoid transfer function in the hidden layer and linear transfer function in the output layer, give us the best performance ($MSE = 3.9629 \times 10^{-4}$, $MAPE = 1.8922\%$ and $R^2 = 0.99835$). Based on the sensitivity analysis, we found that all the input variables have a significant effect on the estimation of fouling resistance.

The validity of the ANN-MLP model is shown compared with two proposed correlations in literature at two different temperature surfaces (wall) for the heat exchanger and with the experimental results of fouling resistance for various times.

Hence, it is concluded that the ANN-MLP model developed in this work can be successfully employed to provide an accurate prediction of the fouling resistance.

ACKNOWLEDGEMENTS

We are grateful to the Laboratory of Biomaterials and Transport Phenomena (LBMPT) of the University of Medea, Birine Nuclear Research Center (CRNB) and DGRSDT.

DATA AVAILABILITY STATEMENT

All relevant data are included in the paper or its Supplementary Information.

REFERENCES

Abdallahelhadj, A., Laidi, M., Si-Moussa, C. & Hanini, S. 2017 Novel approach for estimating solubility of solid drugs in supercritical carbon dioxide and critical properties using direct and inverse artificial neural network (ANN). *Neural Computing and Applications* **28** (1), 87–99.

Al-Janabi, A., Malayeri, M. R. & Müller-Steinhagen, H. 2011 Minimization of $CaSO_4$ deposition through surface modification. *Heat Transfer Engineering* **32** (3–4), 291–299.

Ammi, Y., Khaouane, L. & Hanini, S. 2020 A comparison of neural networks and multiple linear regressions models to describe the rejection of micropollutants by membranes. *Kemija u Industriji* **69** (3–4), 111–127.

Awais, M. & Bhuiyan, A. A. 2019 Recent advancements in impedance of fouling resistance and particulate depositions in heat exchangers. *International Journal of Heat and Mass Transfer* **141**, 580–603.

Belmadani, S., Hanini, S., Laidi, M., Si-Moussa, C. & Hamadache, M. 2020 Artificial neural network models for prediction of density and kinematic viscosity of different systems of biofuels and their blends with diesel fuel. comparative analysis. *Kemija u Industriji* **69** (7–8), 355–364.

Benimam, H., Moussa, C. S., Hentabli, M., Hanini, S. & Laidi, M. 2020 Dragonfly-support vector machine for regression modeling of the activity coefficient at infinite dilution of solutes in imidazolium ionic liquids using σ-profile descriptors. *Journal of Chemical & Engineering Data* **65** (6), 3161–3172.

Bouali, A., Hanini, S., Mohammedi, B. & Boumahdi, M. 2020 Using artificial neural network for predicting heat transfer coefficient during flow boiling in an inclined channel. *Thermal Science* (00), 238-238.

Demuth, H. & Beale, M. 2009 *Matlab Neural Network Toolbox user's Guide Version 6*. The MathWorks Inc., Natick, MA, USA.

Garson, D. G. 1991 Interpreting Neural Network Connection Weights. *AI Expert* **6** (4), 46–51.

Ghahdarijani, A. M., Hormozi, F. & Asl, A. H. 2017 Convective heat transfer and pressure drop study on nanofluids in double-walled reactor by developing an optimal multilayer perceptron artificial neural network. *International Communications in Heat and Mass Transfer* **84**, 11–19.

Grandgeorge, S., Jallut, C. & Thonon, B. 1998 Particulate fouling of corrugated plate heat exchangers. Global kinetic and equilibrium studies. *Chemical Engineering Science* **53** (17), 3050–3071.

Kiani, M. K. D., Ghobadian, B., Tavakoli, T., Nikbakht, A. M. & Najafi, G. 2010 Application of artificial neural networks for the prediction of performance and exhaust emissions in SI engine using ethanol-gasoline blends. *Energy* **35** (1), 65–69.

Kukulka, D. J. & Devgun, M. 2007 Fluid temperature and velocity effect on fouling. *Applied Thermal Engineering* **27** (16), 2732–2744.

Kumari, A., Das, S. K. & Srivastava, P. K. 2014 A neural network model for quantitative prediction of oxide scale in water walls of an operating Indian coal fired boiler. *Research and Review in Electrochemistry* **5**, 155–168.

Laidi, M. & Hanini, S. 2013 Optimal solar COP prediction of a solar-assisted adsorption refrigeration system working with activated carbon/methanol as working pairs using direct and inverse artificial neural network. *International Journal of Refrigeration* **36** (1), 247–257.

Mohamedi, B., Hanini, S., Ararem, A. & Mellel, N. 2015 Simulation of nucleate boiling under ANSYS-FLUENT code by using RPI model coupling with artificial neural networks. *Nuclear Science and Techniques* **26** (4), 40601–040601.

Mohanraj, M., Jayaraj, S. & Muraleedharan, C. 2012 Applications of artificial neural networks for refrigeration, air-conditioning and heat pump systems – a review. *Renewable and Sustainable Energy Reviews* **16** (2), 1340–1358.

Nikkhah, V., Sarafraz, M. M., Hormozi, F. & Peyghambarzadeh, S. M. 2015 Particulate fouling of CuO–water nanofluid at isothermal diffusive condition inside the conventional heat exchanger-experimental and modeling. *Experimental Thermal and Fluid Science* **60**, 83–95.

Ojaniemi, U., Riihimäki, M., Manninen, M. & Pättikangas, T. 2012 Wall function model for particulate fouling applying XDLVO theory. *Chemical Engineering Science* **84**, 57–69.

Peyghambarzadeh, S. M., Vatani, A. & Jamialahmadi, M. 2012 Experimental study of micro-particle fouling under forced convective heat transfer. *Brazilian Journal of Chemical Engineering* **29** (4), 713–724.

Peyghambarzadeh, S. M., Vatani, A. & Jamialahmadi, M. 2013 Influences of bubble formation on different types of heat exchanger fouling. *Applied Thermal Engineering* **50** (1), 848–856.

Prodanovic, V., Fraser, D. & Salcudean, M. 2002 Bubble behavior in subcooled flow boiling of water at low pressures and low flow rates. *International Journal of Multiphase Flow* **28** (1), 1–19.

Rezrazi, A., Hanini, S. & Laidi, M. 2016 An optimisation methodology of artificial neural network models for predicting solar radiation: a case study. *Theoretical and Applied Climatology* **123** (3–4), 769–783.

Ross, T. 1996 Indices for performance evaluation of predictive models in food microbiology. *Journal of Applied Bacteriology* **81** (5), 501–508.

Sarafraz, M. M. & Hormozi, F. 2014 Convective boiling and particulate fouling of stabilized CuO-ethylene glycol nanofluids inside the annular heat exchanger. *International Communications in Heat and Mass Transfer* **53**, 116–123.

Setoodeh, H., Keshavarz, A., Ghasemian, A. & Nasouhi, A. 2015 Subcooled flow boiling of alumina/water nanofluid in a channel with a hot spot: an experimental study. *Applied Thermal Engineering* **90**, 384–394.

Soleimani, R., Shoushtari, N. A., Mirza, B. & Salahi, A. 2013 Experimental investigation, modeling and optimization of membrane separation using artificial neural network and multi-objective optimization using genetic algorithm. *Chemical Engineering Research and Design* **91** (5), 883–903.

Tang, S. Z., Li, M. J., Wang, F. L., He, Y. L. & Tao, W. Q. 2020 Fouling potential prediction and multi-objective optimization of a flue gas heat exchanger using neural networks and genetic algorithms. *International Journal of Heat and Mass Transfer* **152**, 119488.

Teng, K. H., Kazi, S. N., Amiri, A., Habali, A. F., Bakar, M. A., Chew, B. T. & Khan, G. 2017 Calcium carbonate fouling on double-pipe heat exchanger with different heat exchanging surfaces. *Powder Technology* **315**, 216–226.

Wang, J., Xu, Z., Han, Z. & Zhao, Y. 2018 Effect of heat flux and inlet temperature on the fouling characteristics of nanoparticles. *Chinese Journal of Chemical Engineering* **26** (3), 623–630.

Wang, S., Xu, Z. & Wang, J. 2019 Fouling characteristics of MgO particles under subcooled flow boiling. *Journal of Mechanical Science and Technology* **33** (3), 1399–1407.

Williamson, R., Newson, I. & Bott, T. R. 1988 The deposition of haematite particles from flowing water. *The Canadian Journal of Chemical Engineering* **66** (1), 51–54.

Zhan, F., Tang, J., Ding, G. & Zhuang, D. 2016 Experimental investigation on particle deposition characteristics of wavy fin-and-tube heat exchangers. *Applied Thermal Engineering* **99**, 1039–1104.

First received 4 May 2021; accepted in revised form 16 June 2021. Available online 29 June 2021